

Article

Cysteine-Rich Receptor-Like Kinase Gene Family Identification in the *Phaseolus* Genome and Comparative Analysis of Their Expression Profiles Specific to Mycorrhizal and Rhizobial Symbiosis

Elsa-Herminia Quezada ¹ , Gabriel-Xicoténcatl García ¹, Manoj-Kumar Arthikala ¹, Govindappa Melappa ² , Miguel Lara ³ and Kalpana Nanjareddy ^{1,*}

¹ Ciencias Agrogenómicas, Escuela Nacional de Estudios Superiores Unidad León—Universidad Nacional Autónoma de México (UNAM), C.P. 37684 León, Mexico; qrelsa@gmail.com (E.-H.Q.); garxga@gmail.com (G.-X.G.); manoj@enes.unam.mx (M.-K.A.)

² Department of Biotechnology, Dayananda Sagar College of Engineering, Shavige Malleshwara Hills, Kumaraswamy Layout, Bengaluru 560 078, India; drgovindappa-bt@dayanandasagar.edu

³ Departamento de Biología Molecular de Plantas, Instituto de Biotecnología, Universidad Nacional Autónoma de México (UNAM), C.P. 62271 Cuernavaca, Mexico; mflara@ibt.unam.mx

* Correspondence: kalpana@enes.unam.mx; Tel.: +52-477-194-0800 (ext. 43462)

Received: 20 December 2018; Accepted: 9 January 2019; Published: 17 January 2019



Abstract: Receptor-like kinases (RLKs) are conserved upstream signaling molecules that regulate several biological processes, including plant development and stress adaptation. Cysteine (C)-rich receptor-like kinases (CRKs) are an important class of RLK that play vital roles in disease resistance and cell death in plants. Genome-wide analyses of CRK genes have been carried out in *Arabidopsis* and rice, while functional characterization of some CRKs has been carried out in wheat and tomato in addition to *Arabidopsis*. A comprehensive analysis of the CRK gene family in leguminous crops has not yet been conducted, and our understanding of their roles in symbiosis is rather limited. Here, we report the comprehensive analysis of the *Phaseolus* CRK gene family, including identification, sequence similarity, phylogeny, chromosomal localization, gene structures, transcript expression profiles, and in silico promoter analysis. Forty-six CRK homologs were identified and phylogenetically clustered into five groups. Expression analysis suggests that *PvCRK* genes are differentially expressed in both vegetative and reproductive tissues. Further, transcriptomic analysis revealed that shared and unique CRK genes were upregulated during arbuscular mycorrhizal and rhizobial symbiosis. Overall, the systematic analysis of the *PvCRK* gene family provides valuable information for further studies on the biological roles of CRKs in various *Phaseolus* tissues during diverse biological processes, including *Phaseolus*-mycorrhiza/rhizobia symbiosis.

Keywords: common bean; CRKs; Cysteine (C)-rich receptor-like kinases; genome-wide identification; legume; mycorrhizal fungi; *Phaseolus*; *Rhizobium*; RLK

1. Introduction

Plants encounter many environmental cues during their lifespan. The sessile nature of plants exposes them to a broad range of pathogens, nematodes and symbionts. Plants have developed sophisticated mechanisms to defend themselves against pathogenic and parasitic attacks by evoking their immune responses; however, they establish symbiotic associations with the microorganisms via an equally efficient strategy. The plasma membrane localized receptor-like kinases (RLKs) are the key players in perceiving and transducing these external stimuli to further activate the associated

downstream signaling pathways. For instance, RLK elicitation by pathogen/microbe-associated molecular patterns (PAMPs/MAMPs), such as bacterial flagellin or fungal chitin heptamers and octamers, or of host-derived damage-associated molecular patterns (DAMPs), activate the defense pathway. During symbiosis, rhizobia derived lipochito-oligosaccharide (LCO) signals (nodulation Factors) and arbuscular mycorrhizal fungi secreted LCO [1] and short-chain chitin oligomer signals (Cos) [2] (Myc factors) bind to the symbiosis specific RLKs that trigger symbiosis signaling. RLKs are categorized into several sub-families, including leucine-rich repeat RLKs (LRR-RLKs), cysteine-rich repeat (CRR) RLKs (CRKs), domain of unknown function 26 RLKs, S-domain RLKs, and others [3].

Cysteine (C)-rich receptor-like kinases (CRKs), also known as DUF26 RLKs, are a large sub-family of plant RLKs. CRKs have a typical RLK domain structure, i.e., they contain an extracellular domain responsible for signal perception, a single-pass transmembrane domain, and a conserved intracellular serine/threonine (Ser/Thr) protein kinase domain responsible for signal transduction. Most CRKs possess two copies of DUF26 in their extracellular domain. The DUF26 domain contains three conserved cysteine residues in a C-X₈-C-X₂-C configuration [4]. The cysteine residues in each DUF26 domain are predicted to form two cysteine bridges, which are hypothesized to be targeted for apoplastic redox modification [5]. The structure of CRKs suggests the role of the extracellular domain in the perception of extracellular ligand and transmitting the signal to intracellular kinase domains. There are over 40 CRK genes in rice [6] and 44 CRK members in *Arabidopsis* [4,7]. The DUF26 domain is found in at least 50 secreted *Arabidopsis* proteins and in eight *Arabidopsis* plasmodesmata-located proteins (PDLs) [5,8]. Unlike CRKs, the PDL proteins resemble receptor-like proteins, but without the intracellular kinase domain. PDLs are involved in regulating important cellular processes such as plant cell-to-cell communication, viral cell-to-cell movement, and plant immunity [8–10].

CRKs are transcriptionally induced in response to abiotic stress conditions such as salicylic acid, ozone, UV light, drought, and salt treatments [5,11–14]. Likewise, a group of CRKs are also found to specifically respond to pathogens and PAMP treatments [5,13]. Overexpression of *Arabidopsis* CRK4, CRK6, and CRK36 enhanced the activation of early and late PAMP-triggered immunity (PTI) responses and enhanced resistance to the bacterial pathogen *Pseudomonas syringae* pv *tomato* [14]. Overexpression of CRK4, CRK5, CRK13, CRK19, and CRK20 leads to hypersensitive response-associated cell death in transgenic *Arabidopsis* [11,12,15]. CRK7 has been reported to mediate the responses to extracellular reactive oxygen species production [16]. Recent reports suggest involvement of *Arabidopsis* CRK28 and CRK29 responsible for cell death in association with membrane receptor like protein kinase BAK1 in response to *Pseudomonas syringae* infection [17]. CRK family members in *Glycine max* were found to be transcriptionally regulated by the biotic stress signals triggering plant immune response [18]. Further, CRK18 in *Gossypium barbadense* is reported to confer resistance to verticillium wilt resistance [19].

Several RLKs have been implicated in legume symbiosis [20–25]. However, *SymCRK* in *Medicago truncatula* is the only known CRK with a role during symbiosis [26,27]. Although recent years have seen considerable information being generated to understand the gamut of activities of CRKs, little is being done towards understanding the role of CRK genes during legume symbiotic associations.

In the present work, we identified the CRK gene family members in *Phaseolus vulgaris* and compared their expression levels specific to mycorrhizal and rhizobial symbiosis. Further, a detailed analysis of chromosomal localization and phylogenetic relationship among them was carried out. Towards an attempt to understand the phylogenetic distribution of *PvCRK* family members, gene structural analysis, i.e., intron–exon structure, protein secondary structure, conserved motifs, transmembrane helices, and hydrophobicity were studied. Further, the putative function of each *PvCRK* was predicted based on the *cis*-acting elements of the promoters. Expression patterns of *PvCRK* members in various *Phaseolus* tissues were studied. Finally, CRK expression patterns from mycorrhiza/*Rhizobium* inoculated *Phaseolus* roots are studied using previously generated RNA sequencing (RNA-Seq) data. With these analyses, we provide fundamental data for CRK family genes in *P. vulgaris* that could be further applied to studying various biological aspects of CRKs in *Phaseolus*, including symbiosis.

2. Materials and Methods

2.1. Identification, Alignment and Phylogenetic Analysis of CRK Orthologs

The *Arabidopsis* CRK gene family sequences [4] were used as query sequences in BLASTN and BLASTP searches of CRK homologs in *P. vulgaris*, *G. max*, *M. truncatula*, *Oryza sativa* and *Zea mays* in the Phytozome genome database (<https://phytozome.jgi.doe.gov>) using default settings for *e*-value and the number of hit sequences. The genome versions used for different species were *P. vulgaris* v2.1, *Z. mays* PH207 v1.1, *M. truncatula* Mt4.0v1, *O. sativa* v7_JGI and *G. max* Wm82.a2.v1. In addition to Phytozome, various other genome databases were used for the retrieval of CRK homologs, including Legume Information System (<https://legumeinfo.org>) for legumes, Lotus Base (<https://lotus.au.dk>) for *Lotus japonicus*, and OrthoMCL (<http://orthomcl.org>) for *L. japonicus* and *O. sativa*. The respective nucleic acid and peptide sequences were downloaded from the online tool PhytoMine from the plant comparative genomics portal Phytozome v12.1 for further analysis and annotation. Obtained genes and protein sequences were further examined to include the conserved domains by querying using Uniprot [28] and Pfam [29] databases.

Finally, the putative CRK homologs for each species were filtered using conserved sequence motif analyzer MEME [30] (<http://meme-suite.org>) and signal peptide cleavage site predictor SignalP v4.1 [31] (<http://www.cbs.dtu.dk/services/SignalP/>). Multiple sequence alignment of intra-species and *Phaseolus* CRK peptide sequences was performed using ClustalW. Phylogenetic analysis of the aligned sequences was carried out using Molecular Evolutionary Genetics Analysis (MEGA) 7.0 with the neighbor-joining (NJ) method, the JTT+I+G substitution model with 1000 bootstrap replicates keeping the default parameters [32]. Multiple sequence alignment of CRK sequences from individual groups was carried out using ClustalW and further, sequence identity was determined using Sequence Manipulation Suite (http://www.bioinformatics.org/sms2/ident_sim.html).

The chromosomal localization of *P. vulgaris* CRK gene family members were verified from the Phytozome v12.1 database, chromosomal images were drawn using EnsemblPlant tool [33], the centromere positions were designed according to Fonsêca et al. [34] and scale was determined based on Wang et al. [35].

2.2. Analysis of Exon-Intron Structures and Conserved Motif Identification in PvCRK Genes

The exon-intron organization of 46 CRK genes of *Phaseolus* was analyzed using Gene Structure Display Server (GSDS) (<http://gsds.cbi.pku.edu.cn/index.php>) [36]. The conserved motifs of PvCRK family members were determined using Multiple Em for Motif Elicitation (MEME) 4.11.4 (<http://meme-suite.org/tools/meme>). Genes with an *e*-value of $<1 \times 10^{-20}$ were subjected to further analysis. The motif representation was made with MAST version 4.12.0 ordered by *p*-values. The motifs obtained were analyzed with the BLASTP interface at National Center for Biotechnology Information (NCBI) website (<https://blast.ncbi.nlm.nih.gov/Blast>) and Pfam 31.0 database [37]; each was represented by multiple sequence alignments and hidden Markov models (HMMs).

The secondary structures of CRK proteins were predicted by MLRC (Multivariate Linear Regression Combination methods) using SOPMA-GOR4-SIMPA and run in NPS@ server (Network protein sequence analysis) [38]. The output results use the DSSP (Dictionary of protein secondary structure) to describe the structures such as α -helix (Hh) with minimum length 4 residues, extended strand (Ee) in parallel and/or anti-parallel β -sheet conformation.

2.3. Transmembrane Helices and Hydrophobicity Analysis of PvCRK Proteins

Prediction of transmembrane helices of the *P. vulgaris* CRK proteins was achieved by Phobius (<http://phobius.sbc.su.se/>) [39] server utilizing peptide sequences. The hydrophobic character of the CRK proteins was analyzed using ProtScale (<https://web.expasy.org/protscale/>) according to Kyte and Doolittle [40]. The average of hydrophobicity for the 46 CRKs was analyzed with ProtParam (<https://web.expasy.org/protparam/>).

[//web.expasy.org/protparam/](http://web.expasy.org/protparam/)) utilizing the scoring criteria of Gasteiger et al. [41]. The grand average of hydropathicity (GRAVY) value for the proteins was calculated as described by Miao et al. [42].

Next, Plant-mPloc tool (<http://www.csbio.sjtu.edu.cn/bioinf/plant/>) was used to identify the sub-cellular localization of proteins in various cellular organelles and pathways. Plant-mPloc identifies a wide variety of location sites such as cell membrane, cell wall, chloroplast, cytoplasm, endoplasmic reticulum, extracellular, Golgi apparatus, mitochondrion, nucleus, peroxisome, plastid, and vacuole [43].

2.4. Promoter Analysis of CRK Genes and GO Annotation

The promoter regions 2000 bp sequences upstream of coding region of 46 CRK genes were downloaded from Phytozome v12.1, *P. vulgaris* genome database. In silico analysis of promoter sequences was performed using PlantCARE software [44] to identify the *cis*-regulatory elements of CRK promoters. The frequency of the motifs found on each CRK promoter was represented as a pie chart using the R package (<https://www.r-project.org/>).

The Gene Ontology (GO) enrichment analysis was performed using AgriGO and REVIGO online tools (<http://bioinfo.cau.edu.cn/agriGO/>) [45]. GO categories (molecular function, biological process and cellular component) were developed using 46 CRK IDs of *P. vulgaris*. The results are represented graphically.

2.5. Transcriptome Profiling and RT-qPCR Analysis

Previously, we performed global transcriptome profiling in *Phaseolus vulgaris* L. cv. *Negro Jamapa* roots colonized with *Rhizophagus irregularis* spores, or *Rhizobium tropici* strain CIAT899 [46]. The present study utilizes the same transcriptomic data to obtain the expression profiles of CRK family genes under both types of symbiotic conditions. Heat maps were constructed with fold-change values applying the R package (<https://www.r-project.org/>). Venn diagrams were drawn with differentially expressed gene (DEG) numbers using a Venn diagram drawing tool (<http://bioinformatics.psb.ugent.be/webtools/Venn/>).

To validate the RNA-seq data, we surface-sterilized *P. vulgaris* L. cv. *Negro Jamapa* seeds and germinated them as described by Nanjareddy et al. [47]. Two-day-old germinated seedlings were transplanted into sterile vermiculite and were inoculated with *R. irregularis* or *R. tropici* according to Nanjareddy et al. [46]. Uninoculated *P. vulgaris* plants served as controls. Root tissues were separated from the shoots at two-week post inoculation, and were immediately frozen in liquid nitrogen and stored at $-80\text{ }^{\circ}\text{C}$ until they were subjected to RNA extraction. The root tissues were ground in liquid N_2 , and total RNA was extracted using the Spectrum™ Plant Total RNA Kit (Merck KGaA, Darmstadt, Germany) following the manufacturer's recommendations. DNA contamination in the RNA samples were eliminated by incubating the samples with RNase-free DNase ($1\text{ U }\mu\text{L}^{-1}$) at $37\text{ }^{\circ}\text{C}$ for 15 min and then at $65\text{ }^{\circ}\text{C}$ for 10 min. RNA integrity was verified by electrophoresis, and the concentration was assessed using a NanoDrop™ 2000 spectrophotometer (ThermoFisher Scientific, Wilmington, DE, USA). DNA-free RNA samples were used in quantitative real-time PCR assays, which were performed using the iScript™ One-step RT-PCR Kit with SYBR® Green, following the manufacturer's recommendations in an iQ™ 5 (Bio-Rad, Hercules, CA, USA). Each reaction was prepared with 40 ng of RNA as template. A control sample lacked reverse transcriptase (RT) was incorporated to confirm the absence of contaminant DNA. Relative expression values were calculated using the formula $2^{-\Delta\text{CT}}$, where cycle threshold value (ΔCT) is the CT of the gene of interest minus CT of the reference gene. Reference genes *viz.*, *EF1 α* and *IDE* [48,49] were used to normalize the expression data [50]. The gene-specific oligonucleotides used in this study are listed in Supplementary Table S1.

3. Results

3.1. Identification and Phylogenetic Analysis of the CRK Gene Family in *Phaseolus Vulgaris*

Genome-wide identification of CRK genes in *P. vulgaris* was performed based on homology with the identified *Arabidopsis* CRK family genes [5,13]. BLASTN and BLASTP searches were extensively employed to identify *P. vulgaris* CRK homologs from the *P. vulgaris* v2.1 genome database. A total of 46 CRK gene family members were identified in the genome of *P. vulgaris* (Table 1). HMMs of PvCRK proteins were determined based on the presence of two DUF26 domains in the Pfam database. The CRK family members were named according to their chromosome position starting from chromosome one to eleven. The numbering was from the short arm towards the long arm, starting from proximal to distal ends of the respective arms. The length and molecular weight (Mw/Da) of the deduced CRK proteins ranged from 376 to 1072 amino acids and 119.67 kDa to 42.98 kDa, respectively. The theoretical isoelectric point (pI) of most PvCRKs was slightly acidic (4.92–6.95), and twelve CRK proteins were alkaline (7.01–8.11) (Table 1).

Phylogeny of *P. vulgaris* CRK genes was constructed using a NJ method that classified the CRK homologues into two major clusters. One major cluster was divided into three minor clusters/groups and the other into two minor clusters/groups. Hence, the phylogenetic alignment was classified into five groups (Figure 1A). Interestingly, among these groups, 19 out of 22 CRKs localized on chromosome 7 fell into group III and IV. Next, chr11 had a maximum of five CRKs from CRK42 to CRK46, which came under group II of the phylogenetic tree (Figure 1B). Sequence identity of CRK members in each group was found to be 46.5%, 65.15%, 70.29%, 52.37%, and 49.3% in Group I, II, III, IV, and V, respectively.

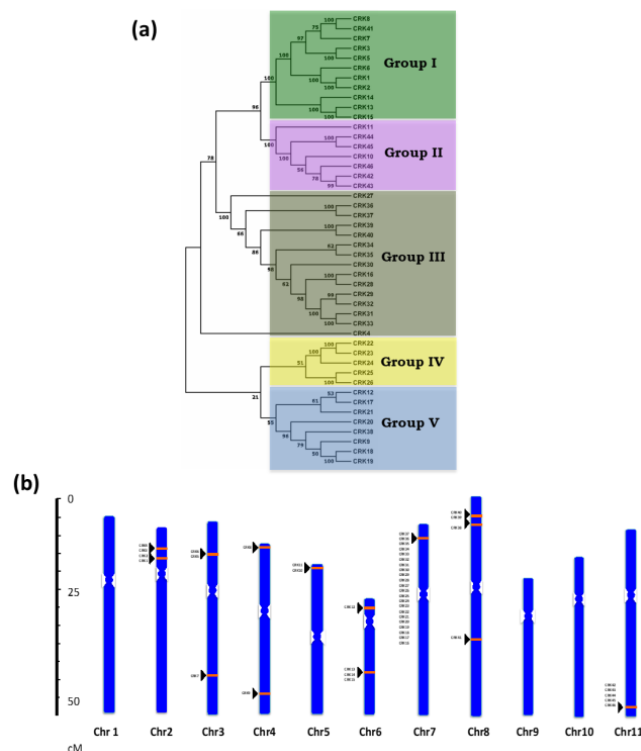


Figure 1. Phylogenetic analysis and chromosomal distribution of *Phaseolus vulgaris* CRK genes. (a) Protein sequences of 46 *P. vulgaris* Cysteine (C)-rich receptor-like kinase (CRK) homologs were identified in the Phytozome database. The phylogenetic tree was constructed using MEGA 7 software with the neighbor-joining (NJ) tree method with 1000 bootstrap values. (b) CRK genes localized to *Phaseolus* chromosomes. The chromosomes are represented by blue bars that are distributed numerically. The orange bands with black triangles indicate the CRK position on the chromosome.

Table 1. The CRK gene family members in *Phaseolus vulgaris*.

Gene ID *	Gene Name §	<i>Arabidopsis</i> Orthologs #	Gene Length, bp	CDS Length, bp	Transcript Length, bp	Protein Length, aa	pI	MW, kDa
PhvuI.002G063900	CRK1	CRK2	3373	1950	2342	649	7.54	72.38
PhvuI.002G063700	CRK2	CRK2	5195	1950	3126	649	7.19	72.23
PhvuI.002G063600	CRK3	CRK2	3272	1632	2114	543	7.54	60.87
		CRK4, CRK5, CRK6, CRK7, CRK8,						
PhvuI.002G049500	CRK4	CRK10, CRK19, CRK20, CRK23	3317	2043	2248	680	6.07	74.88
PhvuI.003G062700	CRK5	CRK3	4054	1968	2501	655	7.18	72.35
PhvuI.003G062600	CRK6	-	3777	1956	2851	651	7.2	72.37
PhvuI.003G020200	CRK7	-	3900	1971	2364	656	7.08	71.53
PhvuI.004G011000	CRK8	CRK42	5206	2013	2326	670	7.22	73.98
PhvuI.004G125200	CRK9	-	3504	2706	2706	901	6.69	102.05
PhvuI.005G015100	CRK10	-	4653	1983	1994	660	5.73	74.05
PhvuI.005G014900	CRK11	-	3863	1986	2278	661	5.47	74.13
PhvuI.006G006800	CRK12	-	2716	1242	1729	413	8.31	47.33
PhvuI.006G084500	CRK13	-	3220	1917	1917	638	6.95	70.81
PhvuI.006G084600	CRK14	-	3385	1941	2206	646	6.81	71.07
PhvuI.006G084800	CRK15	-	4008	1923	1923	640	7.09	70.76
PhvuI.007G052500	CRK16	CRK28	3369	1998	2155	665	4.95	74.96
PhvuI.007G051500	CRK17	-	4473	2004	2004	667	6.78	75.05
PhvuI.007G051300	CRK18	-	4465	2010	2117	669	5.98	75.6
PhvuI.007G051200	CRK19	-	4004	1992	2201	663	6.29	74.91
PhvuI.007G051100	CRK20	-	4031	1944	1970	647	7.43	73.46
PhvuI.007G051000	CRK21	-	3774	1971	2211	656	5.89	73.86
PhvuI.007G050700	CRK22	-	3669	1980	2963	659	6.2	73.28
PhvuI.007G050600	CRK23	-	3272	1986	2377	661	5.84	73.43
PhvuI.007G050500	CRK24	-	4069	2010	2209	669	5.95	74.31
PhvuI.007G050400	CRK25	-	3852	1968	2010	655	5.47	72.69
PhvuI.007G050300	CRK26	-	8823	3219	3219	1072	5.83	119.67
PhvuI.007G050200	CRK27	CRK26	3217	1932	2024	643	6.54	72.12
PhvuI.007G049600	CRK28	CRK28, CRK29	3254	2058	2194	685	4.92	77.23
PhvuI.007G049500	CRK29	CRK28, CRK29	3188	2010	2186	669	5.63	75.25
PhvuI.007G049400	CRK30	CRK28, CRK29	3196	2019	2267	672	5.7	74.77
PhvuI.007G049100	CRK31	CRK28, CRK29	3247	2022	2283	673	5.19	75.84
PhvuI.007G049000	CRK32	CRK28, CRK29	3126	2058	2199	685	5.24	77.2
PhvuI.007G048900	CRK33	CRK28, CRK29	3061	2016	2179	671	5.15	75.69
PhvuI.007G048800	CRK34	CRK28, CRK29	3209	2013	2131	670	5.99	75.27
PhvuI.007G048700	CRK35	CRK26	3389	2001	2351	666	6.92	74.78
PhvuI.007G048600	CRK36	CRK28, CRK29	4596	2052	2307	683	5.13	76.62
PhvuI.007G048500	CRK37	CRK26	5186	2034	2264	677	5.12	76.17
PhvuI.008G077800	CRK38	-	5648	1995	1995	664	7.01	75.18
PhvuI.008G058700	CRK39	CRK28, CRK29	3044	2010	2202	669	5.76	75.13
PhvuI.008G058600	CRK40	CRK28, CRK29	8619	2022	2432	673	5.59	74.92
PhvuI.008G156400	CRK41	CRK42	3969	1995	2462	664	7.51	73.27
PhvuI.011G193300	CRK42	-	2615	1677	2120	558	7.53	63.84
PhvuI.011G194401	CRK43	-	3032	2004	2095	667	6.23	75.46
PhvuI.011G194600	CRK44	-	8175	1890	1953	629	5.81	70.7
PhvuI.011G194700	CRK45	-	5802	1926	1926	641	6.84	72.23
PhvuI.011G196200	CRK46	-	3325	2016	2210	671	6.91	74.98

* Phytozome gene ID; § Nomenclature based on CRK localization on chromosomes (Figure 1B). bp—base pairs; CDS—coding sequence; aa—amino acids; pI—isoelectric point; MW—molecular weight; kDa—kilodaltons.

Phytomine—Inparanoid-Orthomcl.

To investigate the evolutionary relationship between *Phaseolus* CRK proteins and CRKs from other species, a joining–joining method phylogenetic tree was constructed based on full amino acids of CRK family proteins from *P. vulgaris*, *M. truncatula*, *G. max*, *L. japonicus*, *O. sativa*, *Z. mays*, and *A. thaliana*. The dendrogram showed that the 280 CRKs (Table S2) could be classified into 14 distinct groups based on their sequence similarity (Figure S1).

3.2. Localization of CRK Gene Members on *Phaseolus vulgaris* Chromosomes

A total of 46 *PvCRK* genes were mapped to 8 of the 11 *P. vulgaris* chromosomes. The distribution and density of *PvCRK* genes on chromosomes were not uniform (Figure 1B). Among the 11 chromosomes of *P. vulgaris*, chr04, and chr05 contained two CRK genes and chr03 had three genes. Four CRK genes were localized on chr02 and chr08, five genes on chr06 and six genes on chr11. Interestingly, chr07 had a region with high gene density on the short arm, probably due to local gene duplications. The 22 *PvCRK* genes were spread over a genomic region of ~320 kb on chr07, forming the largest CRK gene cluster. CRK genes were absent on chr01, chr09, and chr10. Approximately, 70% of CRK genes were localized on chromosome short arms (Figure 1B).

3.3. Structural Analysis of CRK Genes

To understand the structural features of *Phaseolus* CRKs, we analyzed intron–exon distribution and conserved motifs. Intron–exon location analysis using the GSDS database showed that the number and distribution of intron–exon locations were highly conserved among the CRK homologs in *P. vulgaris* (Figure 2). The CRKs exhibited a range of 4 to 12 exons per gene; among them, 29 genes had 7 exons per gene and most of these also had a conserved distribution and length for each exon. Of 29 CRKs with 7 exons, 20 were localized on chr07 from *CRK16* to *CRK37*, except for *CRK32* with 8 exons and *CRK27*, which had a maximum of 12 exons. Phylogeny of these CRKs also showed grouping of these genes together into group III, IV and V (Figure 1A). In addition, 6 CRKs, *CRK11*, *CRK13*, *CRK14*, *CRK15*, *CRK44*, and *CRK45*, have 8 exons, and *CRK7*, *CRK8*, *CRK41*, and *CRK42* have 6 exons each. The CRK genes that contain 8 and 6 exons were clustered into group I and group II of the phylogenetic tree. *CRK12* had at least 5 exons (Figure 2). However, *CRK27* and *CRK44* had the longest genomic and protein sequence among the 46 *PvCRK* genes (Figures 1A and 2).

The secondary structure prediction of the 46 CRKs in *P. vulgaris* revealed that 29.83% are α -helix, 18.51% are extended strand and 51.65% are random coil. The highest percentage of α -helix was contained in *CRK16* with 40.92%, while *CRK30* showed the lowest amount, with 26.15% α -helix. *CRK46* had the highest percentage of extended strand with 24.19% and *CRK19* had the lowest with 14.99% (Figure S2; Table S3).

3.4. Transmembrane Regions of CRK Proteins

Transmembrane helices were predicted for the 46 CRK proteins in *P. vulgaris* with the Phobius (<http://phobius.sbc.su.se/>) server. All the 46 CRK members of *Phaseolus* were found to contain a single transmembrane domain based on the analysis using Phobius, a combined transmembrane topology and signal peptide predictor. The results confirm that the CRK proteins contained only one transmembrane region typical to CRKs and RLKs (Figure S3). Multiple sequence alignment of *PvCRK* amino acid sequences using ClustalW revealed the highly conserved nature of the transmembrane region in most of the CRKs (Figure S4). The hydrophobicity analysis was carried out to predict whether a peptide segment is sufficiently hydrophobic to interact or reside within the interior of the membrane. The results for the GRAVY outputs showed values ranging from -0.032 to -0.335 for all of the CRK proteins (Table S4). Further, ProtScale analysis was carried out to determine the hydrophobic regions of the CRK proteins (Figure S5); the results agreed with the predicted transmembrane helices (Figure S2).



Figure 2. Gene structure analysis of *Phaseolus* cysteine-rich receptor-like kinases (CRKs). The intron–exon structures of *PvCRK* genes were analyzed using the Gene Structure Display Server (GSDS) database. Exons/Coding sequence (CDS) are represented by orange bars, introns by grey lines, and upstream (5′)/downstream (3′) untranslated regions (UTRs) are blue bars.

3.5. Signal Peptide Analysis and Subcellular Localization of *PvCRK* Proteins

The presence and location of signal peptide cleavage sites in amino acid sequences was predicted using SignalP v4.1; based on a combination of several artificial neural networks, it was determined that all 46 *PvCRK* sequences contained a signal peptide region. The length of signal peptide varied from 19 to 38 amino acids (Figure S3). To investigate the subcellular localization of CRKs, we used Plant-mPloc software to search localization specific motifs. The analysis suggested that all CRKs identified in *Phaseolus* appeared to be localized to plasma membrane.

3.6. Protein Sequence Motif Identification

Conserved motif analysis of the CRK proteins through the MEME server showed seven motifs (Figure 3). The characteristic motif of CRK proteins is DUF26 (Domain unknown function 26; Pfam: PF001657), and alignment of *PvCRK* protein sequences showed two DUF26 domains with the conserved sequence C-X₈-C-X₂-C in most of the *PvCRK*s. However, CRK9 and CRK26 contained four DUF26 domains. The DUF26 domain corresponds to a salt stress response/antifungal activity. Pfam search of other domains showed two kinase domains, PF00069 and PF07714. The remaining four motifs showed no match in the Pfam IDs, and hence their functional role is not understood.

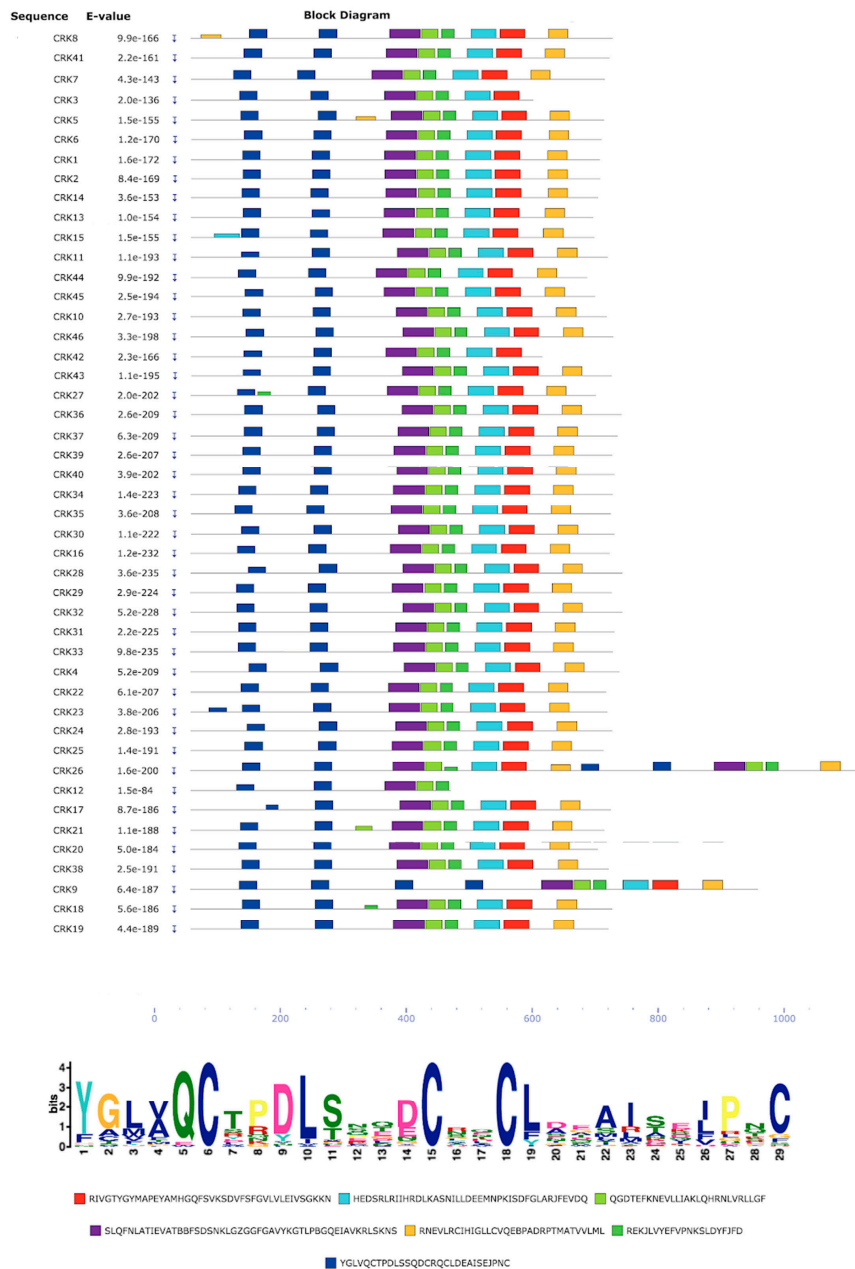


Figure 3. Identification of motifs in CRK protein sequences. MEME was used to identify motifs in the 46 *P. vulgaris* CRKs. Significantly overrepresented motifs are graphically depicted by bars corresponding to their predicted position. The dark blue bars are analogous to salt stress response/antifungal domain (PF01657), and the corresponding sequence logo is shown in the lower section, in which conserved amino acids are represented by one-letter abbreviations. The red boxes represent kinase domains (PF00069) and light blue represents Pkinase_Tyr (PF07714).

3.7. CRK Promoter Analysis

To understand the transcriptional regulation and potential function of the *PvCRK* genes, we analyzed the *cis*-regulatory elements in the promoter sequences (Table S5) using PlantCARE software. The results show 99 motifs for the 2000 bp CRK promoter regions (Table S5). Among them, 20 motifs involved in light response elements, such as ACE, AE-box, AT1-motif, ATCT-motif, Box 4, G-box, GA-motif, GT1-motif, TCT-motif, SP1, and I-box, were important, indicating that the CRK family genes might participate in photosynthesis activity. Several hormonal responsive elements, i.e., auxin responsive AuxRR-core (2 genes) and TGA-element (13 genes); gibberellin response dOCT (1 gene),

GARE-motif (24 genes) and p-box (7 genes); ethylene and ABA responsive ERE (19 genes) and ABRE (19 genes), were also found on the CRK promoter regions (Table S5). Further, CRK promoter regions were also rich in defense, methyl jasmonic acid, and salicylic acid responsive elements. The unique motif ‘fungal elicitor responsive element’ was present on 19 CRK promoters. Notably, TATA box and CAAT box motifs were the most predominant *cis*-regulatory elements found in the CRK promoter regions. The motifs present in the promoter regions of the CRK genes revealed their essential role in growth and development, and in plant-microbe interactions.

Tissue-specific and developmental stage-related expression data provide us with clues about the functions of the *PvCRK* family genes in different vegetative and reproductive tissues of *P. vulgaris*. Therefore, we performed an *in silico* analysis and extracted the expression levels reported in the Phytozome (*P. vulgaris* v2.1) transcriptome database. Based on the expression profile heat map (Figure 4B), we found that an average of 50% CRK genes were downregulated (i.e., Fragments per kilobase of exon model per million reads mapped (FPKM) values > -1.0) in vegetative (roots, stem, leaves, and young trifoliate) and reproductive tissues (flower buds, flower, young pod and mature pod). Upregulated (i.e., FPKM values > 1.0) expression in both vegetative and reproductive tissues was seen in an average of 22% CRK genes. However, the change in transcript expression was not detected in an average of 28% CRKs (Figure 4B). Interestingly, the transcript levels of *CRK4*, *CRK22*, *CRK23*, *CRK29*, *CRK31*, and *CRK40* were highly upregulated, while *CRK9*, *CRK13*, *CRK28*, *CRK38*, and *CRK45* were highly downregulated in all observed tissue types (Figure 4B). Based on most predominant *cis*-regulatory elements found in the CRK promoter regions (Table S5), we selected *CRK16*, *CRK23* and *CRK42* as representative members for the light responsive elements; *CRK2*, *CRK3* and *CRK17* as the defense responsive elements; and *CRK7*, *CRK38*, and *CRK43* as hormonal responsive elements. Next, we performed RT-qPCR analysis for the above selected CRK genes in vegetative and reproductive organs of wild-type *Phaseolus* plants. Differential expression patterns of CRK genes were observed in different *Phaseolus* organs (Figure S5), and these results were consistent with those observed using the *in silico* analysis from the Phytozome (*P. vulgaris* v2.1) transcriptome database (Figure 4B). Together, variable expression patterns were observed among the *PvCRK* members, indicating different functions of CRK genes in various tissues of *P. vulgaris*.

3.8. Gene Ontology and Validation of Transcriptome Data

Gene ontology (GO) was used to classify the 46 CRK genes of *P. vulgaris* into functional groups using AgriGO and REVIGO platforms. Our results show that the CRKs were allocated to three GO categories: biological process, cellular component and molecular function (Figure 5A). Maximum numbers of CRKs were assigned to molecular function (46%), followed by biological processes (43%) and cellular components (11%). In the molecular function category, catalytic activity (GO-0003824), binding (GO-0005488), transferase activity (GO-0016740), and nucleotide binding (GO-0000166) were the most highly represented GO terms. Minor subgroups in the molecular function category included protein kinase activity (GO-0004672), kinase activity (GO-0016301), and phosphotransferase activity (GO-0016773) and transferase activity: transferring phosphorus-containing groups (GO-0016772). In the biological process category, primary metabolic process (GO-0044238), metabolic process (GO-0008152), cellular metabolic process (GO-0044237), cellular process (GO-0009987), cellular macromolecule metabolic process (GO-0044260), and macromolecule metabolic process (GO-0043170) were the most abundant terms. Minor groups within this category included macromolecule modification (GO-0043412), protein phosphorylation (GO-0006468), phosphorylation (GO-0016310), and cellular protein modification process (GO-0006464). In the cellular component category, the most abundant groups were plasma membrane (GO-0005886), cell (GO-0005623) and cell part (GO-0044464). Endomembrane system (GO-0012505) was the only minor group found within this category. The GO functional annotations of the CRKs suggest that the members of the gene family were distributed among several important groups of all three GO categories at distinctive percentages.

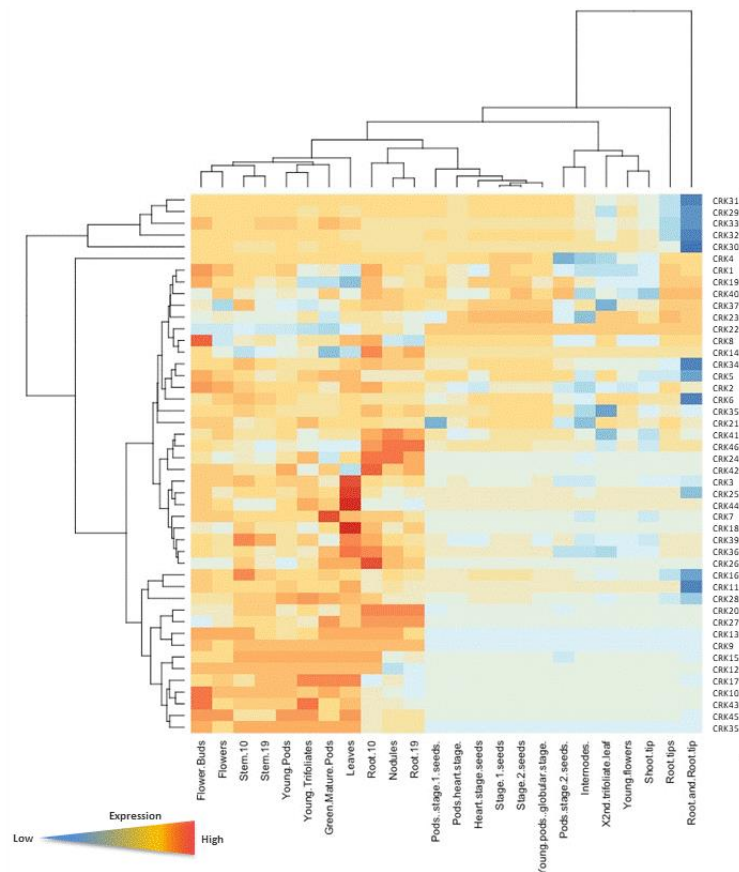


Figure 4. In silico expression profiles of *P. vulgaris* CRKs. Heat map expression profiles of CRK family genes in various tissues of *P. vulgaris*. The transcriptome data across different tissues were extracted by Phytozome (*P. vulgaris* v2.1) and the *P. vulgaris* gene expression atlas (PvGEA). The heat map was generated by R using the Fragments per kilobase of exon model per million reads mapped (FPKM) values of each CRK gene.

Previously, we performed *P. vulgaris* RNA-seq analysis of mRNA from uninoculated control and 2 weeks post inoculation with mycorrhized or nodulated roots using Ion Proton sequencing; data obtained were then deposited in the NCBI with accession number of PRJNA388751 (<https://www.ncbi.nlm.nih.gov/bioproject/388751>). In total, 1959 upregulated and 1260 downregulated mycorrhized DEGs and 1247 upregulated and 1398 downregulated nodulated DEGs were identified [47]. Herein, we validated the RNA-Seq results. Five genes with specific expression patterns under corresponding symbiotic condition were selected for RT-qPCR analysis, and then these results were compared with the previously published transcriptomic data [47] obtained through RNA-Seq. First, the wild-type *P. vulgaris* plants were inoculated with *R. irregularis* or *R. tropici*, and total RNA was isolated 2 weeks postinoculation. Later, the transcript abundance of *CRK3*, *CRK12*, *PvPT4* (*P. vulgaris* phosphate transporter 4), *EnodL12* (early nodulin-like 12) and transcription factor *Myb73* was measured by RT-qPCR analysis. The results obtained from both RT-qPCR and RNA-Seq analyses were found to be same (Figure 5B,C). *CRK3* expression was specific in mycorrhized roots whereas, *CRK12* expression was restricted to nodulated roots. Mycorrhizal symbiosis-specific *PvPT4* expression levels were significantly induced only in mycorrhized roots; similarly, nodule specific *EnodL12* expression was specific in nodulated roots. The *Myb73* transcription factor characterized as a fungal pathogen *Bipolaris oryzae* resistant gene [51] was downregulated in mycorrhized roots but upregulated in nodulated roots (Figure 5B). Hence, the RNA-seq data was used for the identification of CRK family gene expression during mycorrhizal or rhizobial colonization in this study.

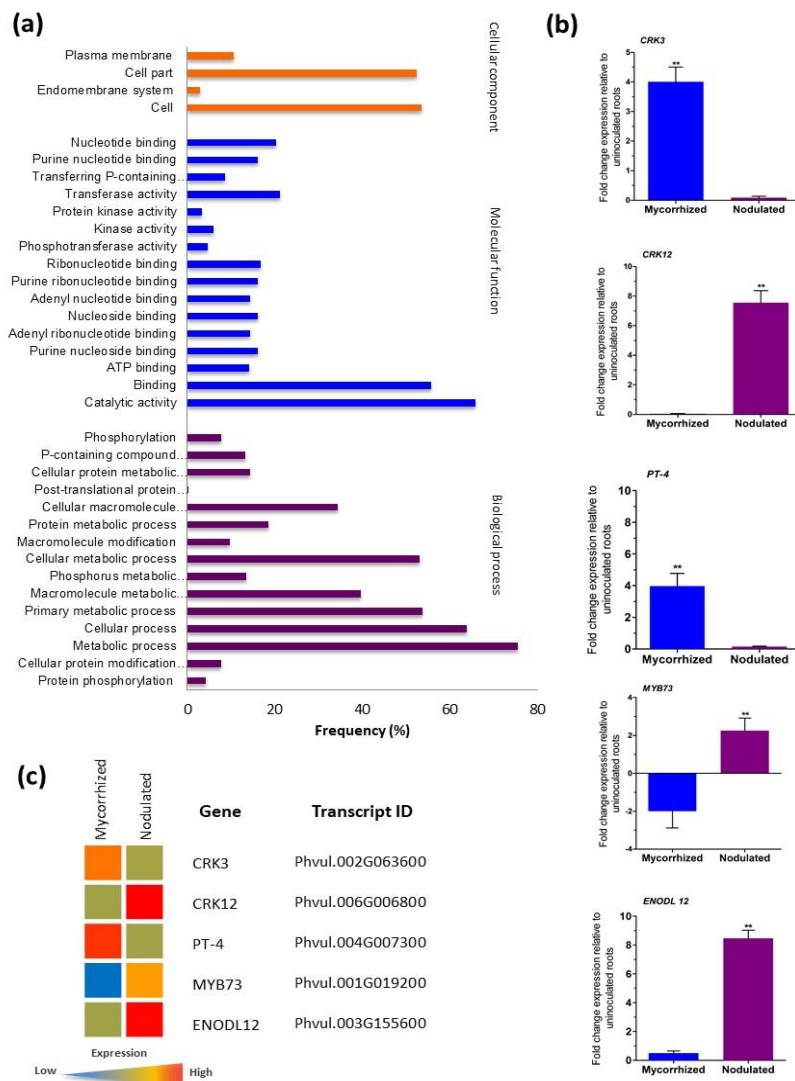


Figure 5. Gene ontology (GO) annotation and RT-qPCR validation of RNA sequencing (RNA-Seq) data from symbiont-colonized *P. vulgaris* roots. (a) GO term annotation of PvCRKs were summarized in three main GO categories, biological process, molecular function and cellular component. GO enrichment analysis performed using AgriGO and REVIGO platforms. Bars indicates the frequency of genes with the same term. (b) RT-qPCR analysis showing relative expression of *Phaseolus CRK3*, *CRK12*, *PT-4*, *MYB73*, and *ENODL12* genes. Candidate genes were selected and corresponding transcript accumulation under mycorrhized and nodulated conditions was quantified by RT-qPCR. RT-qPCR data are the averages of three biological replicates ($n > 9$). Statistical significance of differences between mycorrhized and nodulated roots was determined using an unpaired two-tailed Student's *t*-test (** $p < 0.01$). Error bars represent means \pm Standard error mean (SEM). (c) Heat map of the transcriptomic data obtained through RNA-Seq showing the expression profiles of *CRK3*, *CRK12*, *PT-4*, *MYB73* and *ENODL12*. Color key in red and blue color represents upregulated and downregulated genes respectively whereas, yellow represents no transcript accumulation.

3.9. CRK Gene Expression Patterns in Mycorrhized and Nodulated Roots

During mycorrhizal and rhizobial symbiosis, the host plant recruits specific RLKs to perceive symbiotic signals. CRKs are conserved RLKs across plants and are involved in several key cellular functions. Thus far, the role(s) of CRK family members either in mycorrhizal or rhizobial symbiosis is poorly understood. Herein, based on *P. vulgaris* transcriptomic data [46] we identified differentially expressed CRKs (genes with p -values of ≤ 0.05 and fold-change of ≥ 2.0 (upregulated and

downregulated) were selected). Out of 46 *CRK* family members, we observed 24 and 13 differentially responding *CRK* genes in mycorrhized and nodulated roots, respectively (Figure 6A), indicating that several *CRK* members respond to mycorrhizal colonization compared to nodulation. The Venn diagram intersection and pie chart revealed 17 unique (65%) *CRK* genes (all upregulated) under mycorrhized conditions and 6 unique (16%) *CRK* genes under nodulated conditions (4 *CRK* genes upregulated and 2 downregulated). Seven overlapping (19%) *CRK* genes were found in both the mycorrhizae and rhizobia colonized roots (Figure 6B, Figures S6 and S7). Among the overlapping genes, *CRK37* and *CRK45* were downregulated, whereas *CRK10*, *CRK24*, *CRK27*, *CRK31*, and *CRK44* were upregulated under nodulated conditions. In contrast, all 7 *CRK* genes were upregulated in mycorrhized roots; interestingly *CRK44* was upregulated 7.8-fold compared to 4.9-fold in nodulated roots (Figure 6C). Within the mycorrhized unique genes, *CRK6*, *CRK34*, *CRK35*, and *CRK36* gene transcripts were upregulated over 4-fold and *CRK3*, *CRK11*, *CRK33*, *CRK21*, and *CRK41* were upregulated over 3-fold in mycorrhized roots compared to controls. Among the nodulated unique genes, *CRK12* was upregulated 7.3-fold compared to control roots (Figure 6C).

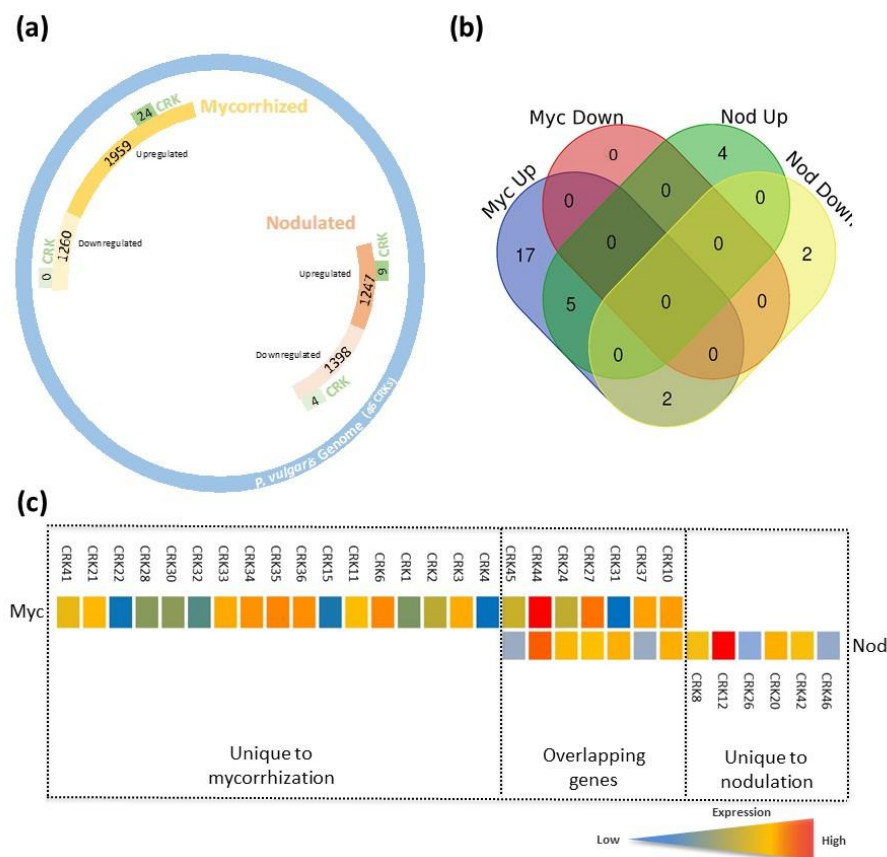


Figure 6. Consolidated representation of genome-wide expression profiling of differentially expressed genes (DEGs) and CRKs in response to root symbionts in *P. vulgaris*. Expression pattern of DEGs in response to mycorrhiza or rhizobia in *P. vulgaris* roots tissues were obtained based on p -values of ≤ 0.05 and fold changes of ≥ 2.0 (upregulated and downregulated). (a) Global transcriptome profile of mycorrhizal fungi and rhizobia activated and repressed genes, and the number of upregulated and downregulated CRKs under each symbiotic condition. (b) Venn diagram showing the number of overlapping expression (upregulated and downregulated) of *CRK* genes in mycorrhized and nodulated roots (clustered into four comparison groups represented by four rounded rectangles) (<http://bioinformatics.psb.ugent.be/webtools/Venn/>). (c) Heat maps showing the unique and overlapping *CRK* gene expression patterns specific to AM and rhizobial colonization. Colour bar shows the fold-change range, with red and blue representing upregulation and downregulation, respectively.

Next, we compared phylogenetic groups with *PvCRK* genes that respond to mycorrhizal and rhizobial colonization. Our observations show that 7, 6, 11, 3, and 3 *CRK* genes were found in Group I, II, III, IV, and V, respectively (Figures 1A and 6C). These combined results indicate that different members of *CRK* family genes are elicited in *P. vulgaris* roots during mycorrhizal and rhizobial symbioses, and the majority belong to the phylogenetic group III.

4. Discussion

Receptor-like kinases are the primary signaling molecules that regulate numerous biological processes, including growth, development and immune responses of plants. CRKs are one of the largest families of RLKs, which have been implicated in abiotic stress, plant defense responses and programmed cell death [11,15,17,52–54]. CRKs have been identified and functionally analyzed in *Arabidopsis* [55,56] rice [6], wheat [57], and tomato [51] to decipher their role in various biological processes. Thus far, legume *SymCRK* has been shown to be involved in *M. truncatula* root nodule symbiosis. Gene characterization studies and functional analysis of *CRK* family genes are needed to elucidate the role of *CRK* family genes. Legume crops are a special class of plants with the unique ability to establish symbiotic association with *Rhizobium* bacteria to fix atmospheric nitrogen and arbuscular mycorrhizal fungi to uptake soil nutrients. Herein, as a first step towards understanding the putative role of CRKs during legume symbiotic associations, we conducted genome-wide identification and expression profiling of the *CRK* gene family in *P. vulgaris*.

In this manuscript, we identified 46 *CRK* members in *Phaseolus*. As in rice and *Arabidopsis*, *CRK* genes were clustered together in the genome of *Phaseolus*. The maximum number of genes in a cluster was on chr07, with 22 CRKs, indicating gene duplications. Gene clusters generally facilitate the recombination and accelerated evolution of the associated traits. Phylogenetic analysis of the *CRK* members resulted in five groups that were based on gene loci, rather than the number of *cys* residues as in case of *Arabidopsis* CRKs. In the present study, we also identified *CRK* family members in *Z. mays* (22 CRKs) and legumes such as *M. truncatula* (47 CRKs), *G. max* (63 CRKs) and *L. japonicus* (18 CRKs) for the first time.

The conserved nature of gene structures in the number of introns–exons and motif compositions further indicated fewer insertions and deletions during evolution and supported the theory of gene duplication. While analyzing the gene structures, the exon numbers were similar on intrachromosomal genes rather than on interchromosomal genes. Most CRKs had two DUF26 domains, except for CRK9 and CRK26, which had four DUF26 domains. Evolutionary patterns are attributed to three mechanisms of gene duplications, including segmental duplication, tandem duplication and transposition events such as retro position and replicative transposition [58]. Segmental duplications are the most frequent occurrence in plants, as they are diploidized polyploids and retain numerous duplicated chromosomal blocks within their genomes [59]. *CRK* gene family analysis in *Phaseolus* shows their distribution in duplicated blocks, implying segmental duplications.

Theoretical isoelectric point analysis revealed that the majority of *PvCRKs* have slightly acidic pH, and the remaining proteins have an alkaline pH. Because plants can vary their gene expression in response to the external pH [60,61], the variation in the isoelectric point of *PvCRKs* could help in the functional diversity of these proteins. The splice variants of the gene families have been shown to have distinct isoelectric points, and the presence of isoforms with varying isoelectric points may help in adaptability to change in external pH [62]. Isoelectric points can also affect protein localization, and hence pI can help in subcellular localization and functionality [63,64]. The analysis of hydrophobicity of CRKs showed negative GRAVY values, which appeared to contradict the hydrophobic nature of membrane localized proteins. Hydropathy analysis showed that *PvCRKs* possess a transmembrane domain whose secondary structure showed alpha helical structures rich in hydrophobic cysteine residues. These alpha helical structures are highly conserved in all *CRK* members identified in *Phaseolus*. In the 3D structure, the hydrophobic cysteine residues will be able to bind to a spectrum of hydrophobic molecules to generate varied cellular responses. Transmembrane proteins contain

hydrophobic midsections within the membrane and hydrophilic ends, which are exposed to the aqueous cellular and extracellular environment. Hence, we would hypothesize that the negative GRAVY values are the average of both hydrophilic and hydrophobic residues in the CRK members.

Cis-regulatory element analysis in promoters of CRK members of *Phaseolus* suggested that they play a role in regulating biotic and abiotic stress responses, and plant growth and development. In the present study, we predicted four types of hormone responsive *cis*-elements in the promoters of *PvCRK* genes, including auxin-responsive, jasmonate-responsive, gibberellin-responsive, ethylene-responsive, and salicylic acid-responsive elements. No motifs related to cytokinin response were detected. In *Arabidopsis*, CRKs are involved in ABA signaling by regulating ABA responses in seed germination, early seedling development and abiotic stress responses. The same *Arabidopsis* study showed plants overexpressing *CRK45* were more sensitive to ABA and hypersensitive to salt and glucose inhibition of seed germination and enhanced drought tolerance, whereas the knockout mutants showed the opposite phenotypes [52,53]. Light responsive *cis*-regulatory elements are another common motif encountered in the promoters of most of the *PvCRKs*. *CRK5* in *Arabidopsis* is the regulator of UV light responses [7]. Defense response elements were common in *PvCRK* promoters, which explain their involvement in hypersensitive response, cell death, and disease resistance in *Arabidopsis* [11,12,15]. Although the promoter analysis of *PvCRKs* did not show symbiosis associated *cis*-elements, the presence of fungal elicitor responsive elements signals the putative role of CRKs during mycorrhizal symbiosis. Nevertheless, previous studies demonstrate phytohormones playing crucial roles in defining the rhizobial and mycorrhizal symbiosis. Auxin regulates nodule development by modulating cell divisions and cell cycle genes in *L. japonicas* and *M. truncatula* [65,66]. The cytokinin receptor CRE1 in *M. truncatula* is known to coordinate nodule organogenesis by integrating bacterial and plant signals [67,68]. Further, abscisic acid is found to coordinate nod factor and cytokinin signaling in *M. truncatula* during nodulation [69]. Although ethylene is an inhibitor of nod factor signal transduction, crosstalk between jasmonic acid and ethylene is essential for the regulation of nodulation [70,71]. Gibberellic acids are also known to play pivotal roles during rhizobia infection and nodule development [72–77]. Similar observations were also made during mycorrhizal symbiosis; auxin perception is known to be required for initiation and arbuscule development by influencing the strigolactones [78–80]. ABA and ethylene were found to influence the AM initiation, colonization and functionality in *M. truncatula* and tomato [81–84]. Further, AM symbiosis was reported to be regulated by gibberellins and GA regulating DELLA proteins [79,85–87].

PvCRK genes show differential expression patterns in various vegetative and reproductive tissues of *Phaseolus*. RT-qPCR analysis of representative *CRK* genes (based on predominant *cis*-regulatory elements for light responsive, defense responsive and hormonal responsive elements) in different *Phaseolus* organs show variable expression patterns and were consistent with the Phytozome transcriptome database. As shown in the results, out of 46 *PvCRKs*, an average of 50% of genes showed low expression and 22% of genes exhibited high expression in all tissues analyzed. Curiously, CRKs with high expression in most of the tissues belonged to phylogenetic group III, implying their indispensable role in various aspects of growth, development, reproduction and defense in homologues in other plant systems [5,7,11–16].

While analyzing the previously reported [47] RNA-Seq data of *Rhizobium*/mycorrhiza inoculated *Phaseolus* for CRK gene expression, interesting facts were uncovered. With the applied cutoff value of the transcripts, 24 *CRK* genes were upregulated and none were specifically downregulated. However, under *Rhizobium* inoculated conditions, 4 *CRK* genes were downregulated and 9 were upregulated. Seven CRKs were shared between the symbiotic conditions. Taken together, 11 CRKs with high expression under mycorrhiza/*Rhizobium* inoculated conditions belonged to group III of the phylogenetic tree of *Phaseolus* CRKs.

5. Conclusions

In summary, we performed a genome-wide analysis of the *CRK* family of *P. vulgaris* and identified 46 *PvCRK* genes. An array of the biochemical characteristics of the *PvCRK* proteins was analyzed. The phylogeny of the *PvCRK* members classified them into five groups, which were substantiated with the similarities found in the gene structure and motif arrangements. *PvCRK* genes were distributed on 8 chromosomes among 11 chromosomes of *Phaseolus*. Gene clustering was the most common feature of the *CRK* gene distribution, and the largest cluster of 22 genes (*CRK16* to *CRK37*) was found on chr07. Gene clustering indicated the possibility of gene duplication as a factor of *CRK* gene family expansion. *PvCRK* members were differentially expressed in all vegetative and reproductive tissues of *P. vulgaris*. Further, GO analysis revealed divergent roles of *CRK* proteins in *Phaseolus*. RNA-Seq data for mycorrhiza/*Rhizobium* colonized *Phaseolus* root tissues revealed shared and unique *PvCRK* genes that could play a decisive role during symbiotic events. This article also provides a comprehensive list of *CRKs* in *L. japonicus*, *M. truncatula* and *G. max* and *Z. mays* as a first report. Taken together, the results provide a foundation for functional characterization of *CRK* proteins in *Phaseolus* and also other species discussed.

Supplementary Materials: The following are available online at <http://www.mdpi.com/2073-4425/10/1/59/s1>, Figure S1: Phylogenetic tree of various *CRK* family genes in legumes and non-legumes. Figure S2: Secondary structure prediction of *CRKs* in *P. vulgaris* by MLRC. Figure S3: Protein structure of *CRKs* in *P. vulgaris*. Figure S4: Multiple sequence alignment of *PvCRK* amino acids using CLUSTAL. Figure S5: Expression patterns of the *CRK* gene in wild-type *P. vulgaris* tissues by RT-qPCR. Figure S6: Hydrophobicity of *P. vulgaris* *CRK* proteins. Figure S7: Pie chart showing the percent of unique and overlapping *CRK* genes during symbioses in *P. vulgaris*. Table S1: Primer sequences of *P. vulgaris* genes used to perform RT-qPCR analyses. Table S2: The comprehensive list of *CRK* transcript IDs of different dicots (legumes and non-legume) and monocots. Table S3: The secondary structure of *Phaseolus vulgaris* *CRK* family proteins. Table S4: List of *Phaseolus* *CRK* proteins showing GRAVY scores. Table S5: In silico analysis of the *Phaseolus vulgaris* *CRK* promoter region.

Author Contributions: M.-K.A. and K.N. conceived and designed the experiments and approved the final manuscript. E.-H.Q. and G.-X.G. performed data collection, bioinformatics analyses and contributed to the experimental design, data analysis and drafted the manuscript. M.G. analyzed the transcriptomic data and statistics. M.L. performed qRT-PCR experiments and coordinated the study. All authors read and approved the manuscript.

Funding: This work was supported by the Dirección General de Asuntos del Personal Académico, DGAPA/PAPIIT-UNAM grant no. IA205117 to M.-K.A. Partially supported by DGAPA/PAPIIT-UNAM grant no. IN219916 to M.L. and DGAPA/PAPIIT-UNAM grant no. IN211218 to K.N.

Acknowledgments: Elsa Herminia Quezada Rodríguez is a doctoral student from Programa de Doctorado en Ciencias Biomédicas, Universidad Nacional Autónoma de México (UNAM) and received fellowship 409344/289810 from CONACYT.

Conflicts of Interest: The authors declare no conflict of interest.

References

- Maillet, F.; Poinso, V.; André, O.; Puech-Pagès, V.; Haouy, A.; Gueunier, M.; Cromer, L.; Giraudet, D.; Formey, D.; Niebel, A.; et al. Fungal lipochitoooligosaccharide symbiotic signals in arbuscular mycorrhiza. *Nature* **2011**, *469*, 58–63. [CrossRef] [PubMed]
- Genre, A.; Chabaud, M.; Balzergue, C.; Puech-Pagès, V.; Novero, M.; Rey, T.; Fournier, J.; Rochange, S.; Bécard, G.; Bonfante, P.; et al. Short-chain chitin oligomers from arbuscular mycorrhizal fungi trigger nuclear Ca^{2+} spiking in *Medicago truncatula* roots and their production is enhanced by strigolactone. *New Phytol.* **2013**, *198*, 190–202. [CrossRef] [PubMed]
- Shiu, S.H.; Bleecker, A.B. Receptor-like kinases from *Arabidopsis* form a monophyletic gene family related to animal receptor kinases. *Proc. Natl. Acad. Sci. USA* **2001**, *98*, 10763–10768. [CrossRef] [PubMed]
- Chen, Z.A. Superfamily of proteins with novel cysteine-rich repeats. *Plant Physiol.* **2001**, *126*, 473–476. [CrossRef] [PubMed]
- Bourdais, G.; Burdiak, P.; Gauthier, A.; Nitsch, L.; Salojärvi, J.; Rayapuram, C.; Idänheimo, N.; Hunter, K.; Kimura, S.; Merilo, E.; et al. Large-Scale phenomics identifies primary and fine-tuning roles for *CRKs* in responses related to oxidative stress. *PLoS Genet.* **2015**, *11*, e1005373. [CrossRef] [PubMed]

6. Chern, M.; Xu, Q.; Bart, R.S.; Bai, W.; Ruan, D.; Sze-To, W.H.; Canlas, P.E.; Jain, R.; Chen, X.; Ronald, P.C. A genetic screen identifies a requirement for cysteine-rich receptor-like kinases in rice NH1 (OsNPR1)-mediated immunity. *PLoS Genet.* **2016**, *12*, e1006049. [[CrossRef](#)]
7. Burdiak, P.; Rusaczonok, A.; Witon, D.; Glów, D.; Karpinski, S. Cysteine-rich receptor-like kinase CRK5 as a regulator of growth, development, and ultraviolet radiation responses in *Arabidopsis thaliana*. *J. Exp. Bot.* **2015**, *66*, 3325–3337. [[CrossRef](#)]
8. Amari, K.; Boutant, E.; Hofmann, C.; Schmitt-Keichinger, C.; Fernandez-Calvino, L.; Didier, F.; Lerich, A.; Mutterer, J.; Thomas, C.L.; Heinlein, M.; et al. A family of plasmodesmal proteins with receptor-like properties for plant viral movement proteins. *PLoS Pathog.* **2010**, *6*, e1001119. [[CrossRef](#)]
9. Lee, J.-Y.; Wang, X.; Cui, W.; Sager, R.; Modla, S.; Czymbek, K.; Zybaliow, B.; van Wijk, K.; Zhang, C.; Lu, H.; et al. A plasmodesmata-localized protein mediates crosstalk between cell-to-cell communication and innate immunity in *Arabidopsis*. *Plant Cell* **2011**, *23*, 3353–3373. [[CrossRef](#)]
10. Caillaud, M.-C.; Wirthmueller, L.; Sklenar, J.; Findlay, K.; Piquerez, S.J.M.; Jones, A.M.E.; Robatzek, S.; Jones, J.D.; Faulkner, C. The plasmodesmal protein PDL1 localises to haustoria-associated membranes during downy mildew infection and regulates callose deposition. *PLoS Pathog.* **2014**, *10*, e1004496. [[CrossRef](#)]
11. Chen, K.; Du, L.; Chen, Z. Sensitization of defense responses and activation of programmed cell death by a pathogen-induced receptor-like protein kinase in *Arabidopsis*. *Plant Mol. Biol.* **2003**, *53*, 61–74. [[CrossRef](#)] [[PubMed](#)]
12. Chen, K.; Fan, B.; Du, L.; Chen, Z. Activation of hypersensitive cell death by pathogen-induced receptor-like protein kinases from *Arabidopsis*. *Plant Mol. Biol.* **2004**, *56*, 271–283. [[CrossRef](#)] [[PubMed](#)]
13. Wrzaczek, M.; Brosché, M.; Salojärvi, J.; Kangasjärvi, S.; Idänheimo, N.; Mersmann, S.; Robatzek, S.; Karpinski, S.; Karpinska, B.; Kangasjärvi, J. Transcriptional regulation of the CRK/DUF26 group of receptor-like protein kinases by ozone and plant hormones in *Arabidopsis*. *BMC Plant Biol.* **2010**, *10*, 95. [[CrossRef](#)] [[PubMed](#)]
14. Yeh, Y.-H.; Chang, Y.-H.; Huang, P.-Y.; Huang, J.-B.; Zimmerli, L. Enhanced *Arabidopsis* pattern-triggered immunity by overexpression of cysteine-rich receptor-like kinases. *Front. Plant Sci.* **2015**, *6*, 322. [[CrossRef](#)] [[PubMed](#)]
15. Acharya, B.R.; Raina, S.; Maqbool, S.B.; Jagadeeswaran, G.; Mosher, S.L.; Appel, H.M.; Schultz, J.C.; Klessig, D.F.; Raina, R. Overexpression of CRK13, an *Arabidopsis* cysteine-rich receptor-like kinase, results in enhanced resistance to *Pseudomonas syringae*. *Plant J.* **2007**, *50*, 488–499. [[CrossRef](#)]
16. Idänheimo, N.; Gauthier, A.; Salojärvi, J.; Siligato, R.; Brosché, M.; Kollist, H.; Mähönen, A.P.; Kangasjärvi, J.; Wrzaczek, M. The *Arabidopsis thaliana* cysteine-rich receptor-like kinases CRK6 and CRK7 protect against apoplastic oxidative stress. *Biochem. Biophys. Res. Commun.* **2014**, *445*, 457–462. [[CrossRef](#)] [[PubMed](#)]
17. Yadeta, K.A.; Elmore, J.M.; Creer, A.Y.; Feng, B.; Franco, J.Y.; Rufian, J.S.; He, P.; Phinney, B.; Coaker, G. A cysteine-rich protein kinase associates with a membrane immune complex and the cysteine residues are required for cell death. *Plant Physiol.* **2016**, *173*, 771–787. [[CrossRef](#)]
18. Delgado-Cerrone, L.; Alvarez, A.; Mena, E.; Ponce de León, I.; Montesano, M. Genome-wide analysis of the soybean CRK-family and transcriptional regulation by biotic stress signals triggering plant immunity. *PLoS ONE* **2018**, *13*, e0207438. [[CrossRef](#)]
19. Li, T.G.; Zhang, D.D.; Zhou, L.; Kong, Z.Q.; Hussaini, A.S.; Wang, D.; Li, J.J.; Short, D.P.; Dhar, N.; Klosterman, S.J.; et al. Genome-wide identification and functional analyses of the CRK gene family in cotton reveals *GbCRK18* confers verticillium wilt resistance in *Gossypium barbadense*. *Front. Plant Sci.* **2018**, *9*, 1266. [[CrossRef](#)]
20. Nishimura, R.; Ohmori, M.; Fujita, H.; Kawaguchi, M. A *Lotus* basic leucine zipper protein with a RING-finger motif negatively regulates the developmental program of nodulation. *Proc. Natl. Acad. Sci. USA* **2002**, *99*, 15206–15210. [[CrossRef](#)]
21. Krusell, L.; Madsen, L.H.; Sato, S. Shoot control of root development and nodulation is mediated by a receptor-like kinase. *Nature* **2002**, *420*, 422–426. [[CrossRef](#)] [[PubMed](#)]
22. Madsen, E.B.; Madsen, L.H.; Radutoiu, S. A receptor kinase gene of the LysM type is involved in legume perception in rhizobial signals. *Nature* **2003**, *425*, 637–640. [[CrossRef](#)] [[PubMed](#)]
23. Radutoiu, S.; Madsen, L.H.; Madsen, E.B. Plant recognition of symbiotic bacteria requires two *LysM* receptor-like kinases. *Nature* **2003**, *425*, 585–592. [[CrossRef](#)] [[PubMed](#)]

24. Limpens, E.; Franken, C.; Smit, P.; Willemse, J.; Bisseling, T.; Geurts, R. *LysM* domain receptor kinases regulating rhizobial Nod factor-induced infection. *Science* **2003**, *302*, 630–633. [[CrossRef](#)] [[PubMed](#)]
25. Parniske, M. Molecular genetics of the arbuscular mycorrhizal symbiosis. *Curr. Opin. Plant Biol.* **2004**, *7*, 414–421. [[CrossRef](#)] [[PubMed](#)]
26. Endre, G.; Kereszt, A.; Kevei, Z.; Mihacea, S.; Kalo, P.; Kiss, G.B. A receptor kinase gene regulating symbiotic nodule development. *Nature* **2002**, *417*, 962–966. [[CrossRef](#)] [[PubMed](#)]
27. Stracke, S.; Kistner, C.; Yoshida, S.; Mulder, L.; Sato, S.; Kaneko, T.; Tabata, S.; Sandal, N.; Stougaard, J.; Szczyglowski, K. A plant receptor-like kinase required for both bacterial and fungal symbiosis. *Nature* **2002**, *417*, 959–962. [[CrossRef](#)]
28. Apweiler, R.; Bairoch, A.; Wu, C.H.; Barker, W.C.; Boeckmann, B.; Ferro, S.; Gasteiger, E.; Huang, H.; Lopez, R.; Magrane, M.; et al. The UniProt Consortium; UniProt: The universal protein knowledgebase. *Nucleic Acids Res.* **2017**, *45*, D158–D169. [[CrossRef](#)]
29. Finn, R.D.; Bateman, A.; Clements, J.; Coggill, P.; Eberhardt, R.Y.; Eddy, S.R.; Heger, A.; Hetherington, K.; Holm, L.; Mistry, J.; et al. Pfam: The protein families database. *Nucleic Acids Res.* **2014**, *42*, D222–D230. [[CrossRef](#)]
30. Bailey, T.L.; Boden, M.; Buske, F.A.; Frith, M.; Grant, C.E.; Clementi, L.; Ren, J.; Wilfred, W.; Noble, W.S. MEME Suite: Tools for motif discovery and searching. *Nucleic Acids Res.* **2009**, *37*, W202–W208. [[CrossRef](#)]
31. Petersen, T.N.; Brunak, S.; von Heijne, G.; Nielsen, H. SignalP 4.0: Discriminating signal peptides from transmembrane regions. *Nat. Methods.* **2011**, *8*, 785–786. [[CrossRef](#)]
32. Kumar, S.; Stecher, G.; Tamura, K. MEGA7: Molecular evolutionary genetics analysis version 7.0 for bigger datasets. *Mol. Biol. Evol.* **2016**, *33*, 1870–1874. [[CrossRef](#)] [[PubMed](#)]
33. Bolser, D.M.; Staines, D.M.; Perry, E.; Kersey, P.J. Ensembl Plants: Integrating tools for visualizing, mining, and analyzing plant genomic data. *Plant Genom. Databases* **2017**, *1533*, 1–31. [[CrossRef](#)]
34. Fonsêca, A.; Ferreira, J.; dos Santos, T.R.B.; Mosiolek, M.; Bellucci, E.; Kami, J.; Gepts, P.; Geffroy, V.; Schweizer, D.; Dos Santos, K.G.B.; et al. Cytogenetic map of common bean (*Phaseolus vulgaris* L.). *Chromosome Res.* **2010**, *18*, 487–502. [[CrossRef](#)] [[PubMed](#)]
35. Wang, S.; Su, J.H.; Beliveau, B.J.; Bintu, B.; Moffitt, J.R.; Wu, C.; Zhuang, X. Spatial organization of chromatin domains and compartments in single chromosomes. *Science* **2016**, *353*, 598–602. [[CrossRef](#)] [[PubMed](#)]
36. Hu, B.; Jin, J.; Guo, A.Y.; Zhang, H.; Luo, J.; Gao, G. GSDS 2.0: An upgraded gene feature visualization server. *Bioinformatics* **2015**, *31*, 1296–1297. [[CrossRef](#)]
37. Finn, R.D.; Coggill, P.; Eberhardt, R.Y.; Eddy, S.R.; Mistry, J.; Mitchell, A.L.; Potter, S.C.; Punta, M.; Qureshi, M.; Sangrador-Vegas, A.; et al. The Pfam protein families database: Towards a more sustainable future. *Nucleic Acids Res.* **2016**, *44*, D279–D285. [[CrossRef](#)] [[PubMed](#)]
38. Guermeur, Y.; Geourjon, C.; Gallinari, P.; Deléage, G. Improved performance in protein secondary structure prediction by inhomogeneous score combination. *Bioinformatics* **1999**, *15*, 413–421. [[CrossRef](#)]
39. Käll, L.; Krogh, A.; Sonnhammer, E.L. A combined transmembrane topology and signal peptide prediction method. *J. Mol. Biol.* **2004**, *338*, 1027–1036. [[CrossRef](#)]
40. Kyte, J.; Doolittle, R.F. ProtScale Tool. *J. Mol. Biol.* **1982**, *157*, 105–132. [[CrossRef](#)]
41. Gasteiger, E.; Hoogland, C.; Gattiker, A.; Duvaud, S.; Wilkins, M.R.; Appel, R.D.; Bairoch, A. Protein Identification and analysis tools on the ExPASy server. In *The Proteomics Protocols Handbook*; John, M.W., Ed.; Humana Press: New York, NY, USA, 2005; pp. 571–607.
42. Miao, L.; Lv, Y.; Kong, L.; Chen, Q.; Chen, C.; Li, J.; Zeng, F.; Wang, S.; Li, J.; Huang, L.; et al. Genome-wide identification, phylogeny, evolution, and expression patterns of *MtN3/saliva/SWEET* genes and functional analysis of *BcNS* in *Brassica rapa*. *BMC Genom.* **2018**, *19*, 174. [[CrossRef](#)]
43. Chou, K.C.; Shen, H.B. Cell-PLoc: A package of web-servers for predicting subcellular localization of proteins in various organisms. *Nat. Protoc.* **2008**, *3*, 153–162. [[CrossRef](#)] [[PubMed](#)]
44. Lescot, M.; Déhais, P.; Thijs, G.; Marchal, K.; Moreau, Y.; Van de Peer, Y.; Rouze, P.; Rombauts, S. PlantCARE, a database of plant *cis*-acting regulatory elements and a portal to tools for in silico analysis of promoter sequences. *Nucleic Acids Res.* **2002**, *30*, 325–327. [[CrossRef](#)] [[PubMed](#)]
45. Tian, T.; Liu, Y.; Yan, H.; You, Q.; Yi, X.; Du, Z.; Xu, W.; Su, Z. agriGO v2.0: A GO analysis toolkit for the agricultural community, 2017 update. *Nucleic Acids Res.* **2017**, *45*, W122–W129. [[CrossRef](#)] [[PubMed](#)]

46. Nanjareddy, K.; Arthikala, M.K.; Gómez, B.M.; Blanco, L.; Lara, M. Differentially expressed genes in mycorrhized and nodulated roots of common bean are associated with defense, cell wall architecture, N metabolism, and P metabolism. *PLoS ONE* **2017**, *12*, e0182328. [[CrossRef](#)] [[PubMed](#)]
47. Nanjareddy, K.; Arthikala, M.K.; Aguirre, A.L.; Gómez, B.M.; Lara, M. Plant promoter analysis: Identification and characterization of root nodule specific promoter in the common bean. *J. Vis. Exp.* **2017**, *130*, e56140. [[CrossRef](#)]
48. Islas-Flores, T.; Guillén, G.; Alvarado-Affantranger, X.; Lara-Flores, M.; Sánchez, F.; Villanueva, M.A. *PvRACK1* loss-of-function impairs cell expansion and morphogenesis in *Phaseolus vulgaris* L. root nodules. *Mol. Plant Microbe Interact.* **2011**, *24*, 819–826. [[CrossRef](#)]
49. Borges, A.; Tsai, S.M.; Caldas, D.G. Validation of reference genes for RT-qPCR normalization in common bean during biotic and abiotic stresses. *Plant Cell Rep.* **2012**, *31*, 827–838. [[CrossRef](#)]
50. Vandesompele, J.; De Preter, K.; Pattyn, F.; Poppe, B.; Van Roy, N.; De Paepe, A.; Speleman, F. Accurate normalization of real-time quantitative RT-PCR data by geometric averaging of multiple internal reference genes. *Genome Biol.* **2002**, *3*. [[CrossRef](#)]
51. Jia, J.; Xing, J.H.; Dong, J.G.; Han, J.M.; Liu, J.S. Functional analysis of *MYB73* of *Arabidopsis thaliana* against *Bipolaris oryzae*. *Sci. Agric. Sin.* **2011**, *10*, 721–727. [[CrossRef](#)]
52. Ederli, L.; Madeo, L.; Calderini, O.; Gehring, C.; Moretti, C.; Buonauro, R.; Paolocci, F.; Pasqualini, S. The *Arabidopsis thaliana* cysteine-rich receptor-like kinase CRK20 modulates host responses to *Pseudomonas syringae* pv. tomato DC3000 infection. *J. Plant Physiol.* **2011**, *168*, 1784–1794. [[CrossRef](#)]
53. Tanaka, H.; Osakabe, Y.; Katsura, S.; Mizuno, S.; Maruyama, K.; Kusakabe, K.; Mizoi, J.; Shinozaki, K.; Yamaguchi-Shinozaki, K. Abiotic stress-inducible receptor-like kinases negatively control ABA signaling in *Arabidopsis*. *Plant J.* **2012**, *70*, 599–613. [[CrossRef](#)] [[PubMed](#)]
54. Zhang, X.; Yang, G.; Shi, R.; Han, X.; Qi, L.; Wang, R.; Xiong, L.; Li, G. *Arabidopsis* cysteine-rich receptor like kinase 45 functions in the responses to abscisic acid and abiotic stresses. *Plant Physiol. Biochem.* **2013**, *67*, 189–198. [[CrossRef](#)] [[PubMed](#)]
55. Lu, K.; Liang, S.; Wu, Z.; Bi, C.; Yu, Y.T.; Wang, X.F.; Zhang, D.P. Overexpression of an *Arabidopsis* cysteine-rich receptor-like protein kinase, CRK5, enhances abscisic acid sensitivity and confers drought tolerance. *J. Exp. Bot.* **2016**, *67*, 5009–5027. [[CrossRef](#)]
56. Lee, D.S.; Kim, Y.C.; Kwon, S.J.; Ryu, C.-M.; Park, O.K. The *Arabidopsis* Cysteine-rich receptor-like kinase CRK36 regulates immunity through interaction with the cytoplasmic kinase BIK1. *Front. Plant Sci.* **2017**, *8*, 1856. [[CrossRef](#)]
57. Yang, K.; Rong, W.; Qi, L.; Li, J.; Wei, X.; Zhang, Z. Isolation and characterization of a novel wheat cysteine-rich receptor-like kinase gene induced by *Rhizoctonia cerealis*. *Sci. Rep.* **2013**, *3*, 3021. [[CrossRef](#)] [[PubMed](#)]
58. Kong, H.; Landherr, L.L.; Frohlich, M.W.; Leebens Mack, J.; Ma, H.; DePamphilis, C.W. Patterns of gene duplication in the plant *SKP1* gene family in angiosperms: Evidence for multiple mechanisms of rapid gene birth. *Plant J.* **2007**, *50*, 873–885. [[CrossRef](#)]
59. Cannon, S.B.; Mitra, A.; Baumgarten, A.; Young, N.D.; May, G. The roles of segmental and tandem gene duplication in the evolution of large gene families in *Arabidopsis thaliana*. *BMC Plant Biol.* **2004**, *4*, 10. [[CrossRef](#)]
60. Lager, I.; Andreasson, O.; Dunbar, T.L.; Andreasson, E.; Escobar, M.A.; Rasmusson, A.G. Changes in external pH rapidly alter plant gene expression and modulate auxin and elicitor responses. *Plant Cell Environ.* **2010**, *33*, 1513–1528. [[CrossRef](#)]
61. Kosova, K.; Vitamvas, P.; Urban, M.O.; Prasil, I.T.; Renaut, J. Plant abiotic stress proteomics: The major factors determining alterations in cellular proteome. *Front. Plant Sci.* **2018**, *9*, 22. [[CrossRef](#)]
62. Brew-Appiah, R.; York, Z.B.; Krishnan, V.; Roalson, E.H.; Sanguinet, K.A. Genome-wide identification and analysis of the *ALTERNATIVE OXIDASE* gene family in diploid and hexaploid wheat. *PLoS ONE* **2018**, *13*, e0201439. [[CrossRef](#)]
63. Schwartz, R.; Ting, C.S.; King, J. Whole proteome pI values correlate with subcellular localizations of proteins for organisms within the three domains of life. *Genome Res.* **2001**, *11*, 703–709. [[CrossRef](#)] [[PubMed](#)]
64. Kiraga, J.; Mackiewicz, P.; Mackiewicz, D.; Kowalczyk, M.; Biecek, P.; Polak, N.; Smolarczyk, K.; Dudek, M.R.; Cebrat, S. The relationships between the isoelectric point and: Length of proteins, taxonomy and ecology of organisms. *BMC Genom.* **2007**, *8*, 16. [[CrossRef](#)] [[PubMed](#)]

65. Suzaki, T.; Yano, K.; Ito, M.; Umehara, Y.; Suganuma, N.; Kawaguchi, M. Positive and negative regulation of cortical cell division during root nodule development in *Lotus japonicus* is accompanied by auxin response. *Development* **2012**, *139*, 3997–4006. [[CrossRef](#)] [[PubMed](#)]
66. Breakspear, A.; Liu, C.; Roy, S.; Stacey, N.; Rogers, C.; Trick, M.; Morieri, G.; Mysore, K.S.; Wen, J.; Oldroyd, G.E.; et al. The root hair “infectome” of *Medicago truncatula* uncovers changes in cell cycle genes and reveals a requirement for auxin signaling in rhizobial infection. *Plant Cell* **2014**, *26*, 4680–4701. [[CrossRef](#)] [[PubMed](#)]
67. Gonzalez-Rizzo, S.; Crespi, M.; Frugier, F. The *Medicago truncatula* CRE1 cytokinin receptor regulates lateral root development and early symbiotic interaction with *Sinorhizobium meliloti*. *Plant Cell* **2006**, *18*, 2680–2693. [[CrossRef](#)] [[PubMed](#)]
68. Plet, J.; Wasson, A.; Ariel, F.; Le Signor, C.; Baker, D.; Mathesius, U.; Crespi, M.; Frugier, F. MtCRE1-dependent cytokinin signaling integrates bacterial and plant cues to coordinate symbiotic nodule organogenesis in *Medicago truncatula*. *Plant J.* **2011**, *65*, 622–633. [[CrossRef](#)]
69. Ding, Y.; Kalo, P.; Yendrek, C.; Sun, J.; Liang, Y.; Marsh, J.F.; Harris, J.M.; Oldroyd, G.E. Abscisic acid coordinates nod factor and cytokinin signaling during the regulation of nodulation in *Medicago truncatula*. *Plant Cell* **2008**, *20*, 2681–2695. [[CrossRef](#)]
70. Oldroyd, G.E.; Engstrom, E.M.; Long, S.R. Ethylene inhibits the Nod factor signal transduction pathway of *Medicago truncatula*. *Plant Cell* **2001**, *13*, 1835–1849. [[CrossRef](#)]
71. Sun, J.; Cardoza, V.; Mitchell, D.M.; Bright, L.; Oldroyd, G.; Harris, J.M. Crosstalk between jasmonic acid, ethylene and nod factor signaling allows integration of diverse inputs for regulation of nodulation. *Plant J.* **2006**, *46*, 961–970. [[CrossRef](#)]
72. Lievens, S.; Goormachtig, S.; Den Herder, J.; Capoen, W.; Mathis, R.; Hedden, P.; Holster, M. Gibberellins are involved in nodulation of *Sesbania rostrata*. *Plant Physiol.* **2005**, *139*, 1366–1379. [[CrossRef](#)]
73. Ferguson, B.J.; Ross, J.J.; Reid, J.B. Nodulation phenotypes of gibberellin and brassinosteroid mutants of pea. *Plant Physiol.* **2005**, *138*, 2396–2405. [[CrossRef](#)] [[PubMed](#)]
74. Ferguson, B.J.; Foo, E.; Ross, J.J.; Reid, J.B. Relationship between gibberellin, ethylene and nodulation in *Pisum sativum*. *New Phytol.* **2011**, *189*, 829–842. [[CrossRef](#)] [[PubMed](#)]
75. Libault, M.; Farmer, A.; Brechenmacher, L.; Drnevich, J.; Langley, R.J.; Bilgin, D.D.; Radwan, O.; Neece, D.J.; Clough, S.J.; May, G.D.; et al. Complete transcriptome of the soybean root hair cell, a single-cell model, and its alteration in response to *Bradyrhizobium japonicum* infection. *Plant Physiol.* **2010**, *152*, 541–552. [[CrossRef](#)] [[PubMed](#)]
76. Hayashi, S.; Reid, D.E.; Lorenc, M.T.; Stiller, J.; Edwards, D.; Gresshoff, P.M.; Ferguson, B.J. Transient Nod factor-dependent gene expression in the nodulation-competent zone of soybean (*Glycine max* [L.] Merr.) roots. *Plant Biotech. J.* **2012**, *10*, 995–1010. [[CrossRef](#)] [[PubMed](#)]
77. Middleton, A.M.; Úbeda-Tomás, S.; Griffiths, J.; Holman, T.; Hedden, P.; Thomas, S.G.; Phillips, A.L.; Holdsworth, M.; Bennett, M.J.; King, J.R.; et al. Mathematical modeling elucidates the role of transcriptional feedback in gibberellin signaling. *Proc. Natl. Acad. Sci. USA* **2012**, *109*, 7571–7576. [[CrossRef](#)] [[PubMed](#)]
78. Hanlon, M.T.; Coenen, C. Genetic evidence for auxin involvement in arbuscular mycorrhizal initiation. *New Phytol.* **2011**, *189*, 701–709. [[CrossRef](#)] [[PubMed](#)]
79. Foo, E.; Ross, J.J.; Jones, W.T.; Reid, J.B. Plant hormones in arbuscular mycorrhizal symbioses: An emerging role for gibberellins. *Ann. Bot.* **2013**, *111*, 769–779. [[CrossRef](#)]
80. Etemadi, M.; Gutjahr, C.; Couzigou, J.-M.; Zouine, M.; Lauressergues, D.; Timmers, A.; Audran, C.; Bouzayen, M.; Becard, G.; Combier, J.-P. Auxin perception is required for arbuscule development in arbuscular mycorrhizal symbiosis. *Plant Physiol.* **2014**, *166*, 281–292. [[CrossRef](#)]
81. Herrera-Medina, M.J.; Steinkellner, S.; Vierheilig, H.; Ocampo, J.A.; García-Garrido, J.M. Abscisic acid determines arbuscule development and functionality in the tomato arbuscular mycorrhiza. *New Phytol.* **2007**, *175*, 554–564. [[CrossRef](#)]
82. Rodriguez, J.A.; Morcillo, R.L.; Vierheilig, H.; Ocampo, J.A.; Ludwig-Müller, J.; Garrido, J.M. Mycorrhization of the *notabilis* and *sitiens* tomato mutants in relation to abscisic acid and ethylene contents. *J. Plant Physiol.* **2010**, *167*, 606–613. [[CrossRef](#)]
83. De Los Santos, R.T.; Vierheilig, H.; Ocampo, J.A.; García-Garrido, J.M. Altered pattern of arbuscular mycorrhizal formation in tomato ethylene mutants. *Plant Signal Behav.* **2011**, *6*, 755–758. [[CrossRef](#)] [[PubMed](#)]

84. Charpentier, M.; Sun, J.; Wen, J.; Mysore, K.S.; Oldroyd, G. ABA promotion of arbuscular mycorrhizal colonization requires a component of the PP2A Protein Phosphatase Complex. *Plant Physiol.* **2014**, *166*, 2077–2090. [[CrossRef](#)] [[PubMed](#)]
85. Floss, D.S.; Levy, J.G.; Lévesque-Tremblay, V.; Pumplin, N.; Harrison, M.J. DELLA proteins regulate arbuscule formation in arbuscular mycorrhizal symbiosis. *Proc. Natl. Acad. Sci. USA* **2013**, *110*, E5025–E5034. [[CrossRef](#)] [[PubMed](#)]
86. Martín-Rodríguez, J.A.; Ocampo, J.A.; Molinero-Rosales, N.; Tarkowská, D.; Ruíz-Rivero, O.; García-Garrido, J.M. Role of gibberellins during arbuscular mycorrhizal formation in tomato: New insights revealed by endogenous quantification and genetic analysis of their metabolism in mycorrhizal roots. *Physiol. Plant* **2015**, *154*, 66–81. [[CrossRef](#)] [[PubMed](#)]
87. Yu, N.; Luo, D.; Zhang, X.; Liu, J.; Wang, W.; Jin, Y.; Dong, W.; Liu, J.; Liu, H.; Yang, W.; et al. A DELLA protein complex controls the arbuscular mycorrhizal symbiosis in plants. *Cell Res.* **2014**, *24*, 130–133. [[CrossRef](#)]



© 2019 by the authors. Licensee MDPI, Basel, Switzerland. This article is an open access article distributed under the terms and conditions of the Creative Commons Attribution (CC BY) license (<http://creativecommons.org/licenses/by/4.0/>).